

# Interface Stabilized Nanoscale Quasi-Liquid Films

Jian Luo<sup>1\*</sup>, Shen J. Dillon<sup>2</sup>, and Martin P. Harmer<sup>3</sup>

<sup>1</sup>School of Materials Science and Engineering, Clemson University, Clemson, SC 29634

<sup>2</sup>Department of Materials Science and Engineering, University of Illinois at Urbana-Champaign, Urbana, IL 61801

<sup>3</sup>Department of Materials Science and Engineering, Lehigh University, Bethlehem, PA 18015

\* jluo@alum.mit.edu

## Introduction

A unique class of impurity-based quasi-liquid films has been widely observed at free surfaces, grain boundaries (GBs), and hetero-phase interfaces in ceramic and metallic materials (Figure 1). These nanometer-thick interfacial films can be alternatively understood to be: (a) quasi-liquid layers that adopt an “equilibrium” thickness in response to a balance of attractive and repulsive interfacial forces (in a high-temperature colloidal theory) or (b) multilayer adsorbates with thickness and average composition set by bulk dopant activities [1-2]. In several model binary systems, such quasi-liquid, interfacial films are found to be thermodynamically stable well below the bulk solidus lines, provoking analogies to the simpler interfacial phenomena of premelting in unary systems [3] and prewetting in binary de-mixed liquids [4]. These interfacial films exhibit structures and compositions that are neither observed nor stable as bulk phases, as well as transport, mechanical, and physical properties that are markedly different from bulk phases.

This overview article briefly reviews recent observations in this field with an emphasis on microscopy results. Reviews for specialists can be found elsewhere [1, 5].

## Premelting in Unary Systems

Premelting, also known as “surface melting,” refers to the stabilization of a thin surface liquid layer below the bulk melting

temperature ( $T_m$ ) in unary systems [3]. This can be conceived as if the increased free energy for forming an undercooled liquid film of thickness  $h$  is more than compensated by the reduction in interfacial energies upon replacing a crystal-vapor interface with a crystal-liquid interface and a liquid-vapor interface:

$$\Delta S_{\text{fusion}}(T_m - T) \cdot h < \gamma_{\text{CV}} - (\gamma_{\text{CL}} + \gamma_{\text{LV}})$$

where  $\Delta S_{\text{fusion}}$  is fusion entropy and the  $\gamma$  parameters are excess interfacial energies. Convincing experimental evidence for premelting has been obtained in ice, lead, and other unary systems.

Premelting is the reason that ice is slippery. We often explain ice skating using a “pressure melting” theory. Quantitatively, however, an ice skater can exert a pressure to cause local melting at only a few degrees below zero [6]. Premelting, along with additional frictional heating, enables us to skate at as low as -35 °C [6]. Furthermore, ice premelting plays important roles in snow “sintering” and glacier motion (creep) [3].

## Surficial Films in Binary Oxides

Impurity-based films of self-selecting (equilibrium) thickness form on the surfaces of various doped oxide nanoparticles [5]. These films are often termed as surficial amorphous films (SAFs), although they generally exhibit partial structural order. For  $V_2O_5$ -based SAFs on  $TiO_2$  anatase {101} surfaces, the film thickness decreases monotonically with decreasing

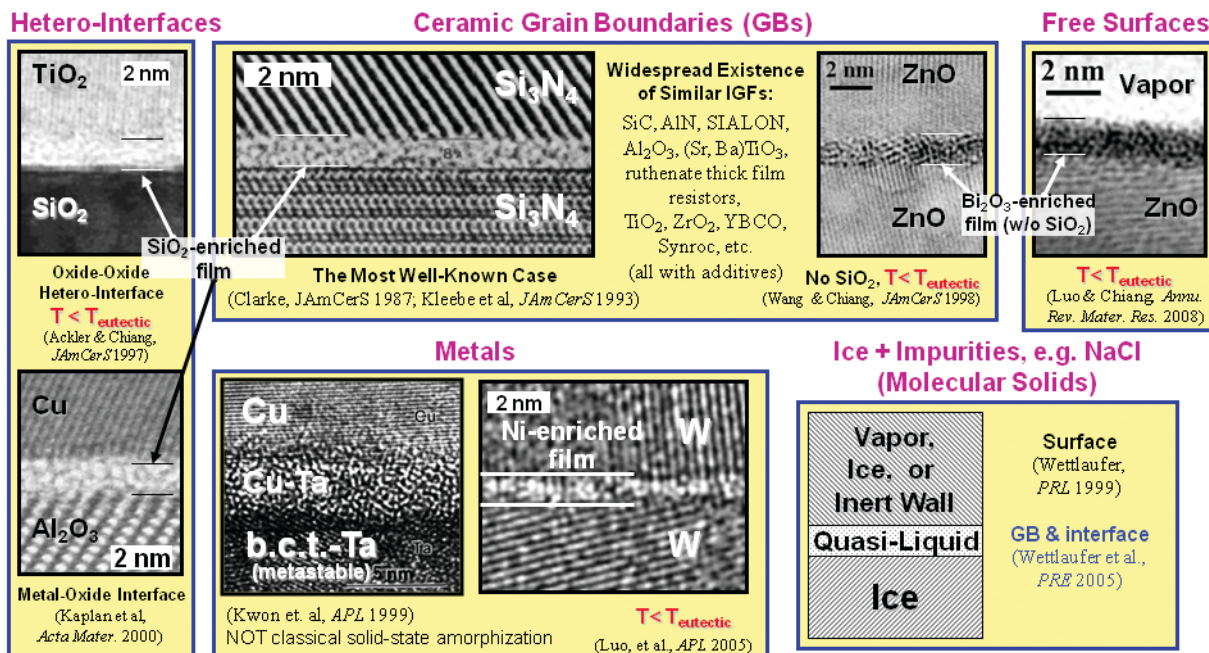


Figure 1: Representative impurity-based quasi-liquid interfacial films. Adapted from Ref. 1 with permission from Taylor & Francis.

# MIRA

## Schottky FE-SEM

Value and Excellence in SEMs



[www.tescan.com](http://www.tescan.com)

- Wide Field Optics™
- In-Flight Beam Tracing™
- In-Beam Detector
- Active Vibration Isolation

All as Tescan standard for the highest-quality imaging

 **TESCAN**  
PERFORMANCE IN NANOSPACE

Tescan USA Inc.  
Web: [www.tescan-usa.com](http://www.tescan-usa.com)  
Email: [info@tescan-usa.com](mailto:info@tescan-usa.com)  
Tel: 724-772-7433

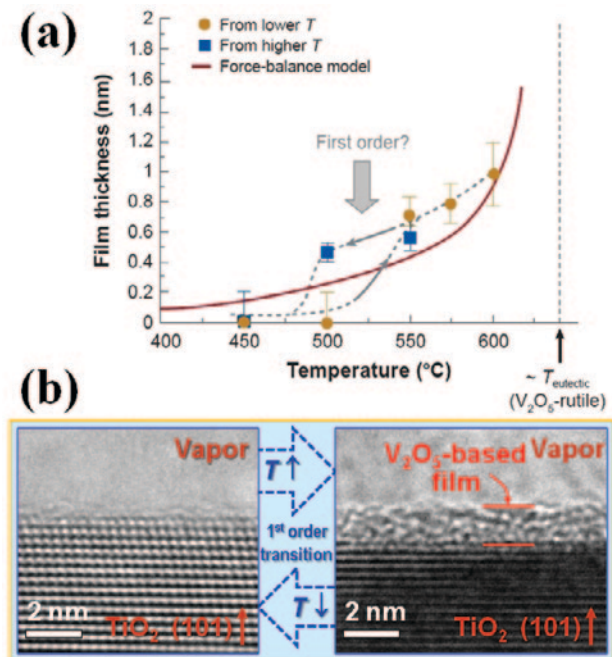


**Figure 2:** (a) Average film thickness vs. equilibration temperature for  $V_2O_5$ -based subsolidus SAFs on  $TiO_2$  anatase (101) facets. (b) Illustration of a reversible first-order surface transition. Adapted from Ref. 7 with permission from Elsevier and AIP.

temperature in the subeutectic regime (Figure 2) and vanishes at a first-order surface transition [7].

For  $Bi_2O_3$  on ZnO, SAF formation is anisotropic: while  $\{11\bar{2}0\}$  facets exhibit SAFs,  $\{1\bar{1}00\}$  facets are devoid of films (Figure 3) [8–11]. In the single-phase and subeutectic two-phase regimes, the thickness of SAFs on the  $\{11\bar{2}0\}$  facets decreases with decreasing temperature or  $Bi_2O_3$  activity [9, 10]. Because of the presence of an attractive London dispersion force, nanoscale quasi-liquid SAFs persist into the solid-liquid two-phase regime,

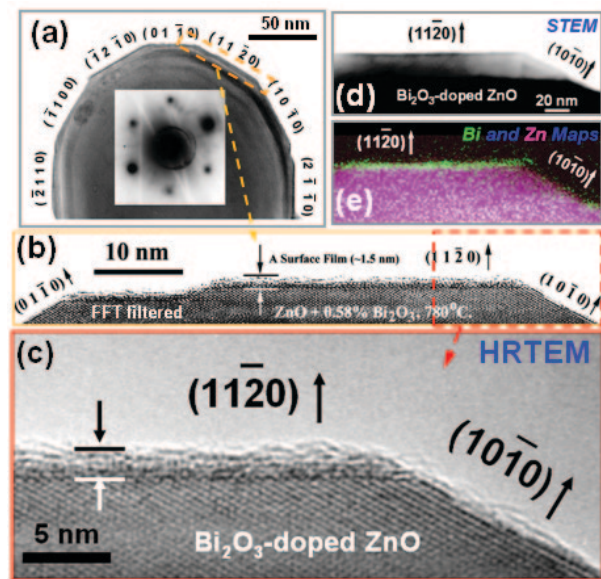


**Figure 3:** (a) TEM image of an anisotropic ZnO nanoparticle with inset diffraction pattern. (b) and (c) HRTEM of several facets, (d) STEM image and, (e) X-ray compositional map of the anisotropic SAF formation. Adapted from Refs. 8 and 9 with permission from Elsevier.

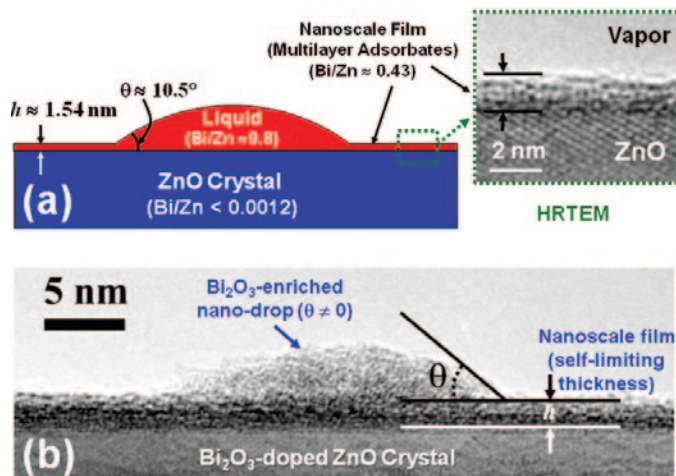


**Figure 4:** (a) Schematic illustration of the equilibrium surface wetting and adsorption configuration for a  $Bi_2O_3$ -rich liquid drop on the ZnO  $\{11\bar{2}0\}$  surface at  $780^\circ\text{C}$  ( $T_{\text{eutectic}} = 740^\circ\text{C}$ ). (b) HRTEM image of a nanometer-thick SAF coexisting with a nanoscale glass droplet at  $700^\circ\text{C}$ . Adapted from Refs. 10 and 11 with permission from Elsevier and ACS.

in equilibrium with partial-wetting bulk liquid drops [11]; yet, the average film composition is markedly different from that of bulk liquid [Figure 4a]. In a few cases, nanometer-thick SAFs are found to co-exist with nanoscale glass or liquid drops with non-zero contact angles [Figure 4b], directly demonstrating the self-limiting thickness. Interested readers are referred to a recent review article on SAFs [5].

### Intergranular Films in Ceramics and Metals

Impurity-based nanoscale intergranular films (IGFs) have been widely observed in ceramics (Figure 1). Clarke originally proposed that these IGFs exhibit an equilibrium thickness [12]. A recent review article [1] summarizes the observations and theories of IGFs.

SAFs are considered as the free-surface counterparts to IGFs in ceramics. On the other hand, metallic counterparts to the ceramic IGFs have also been observed in Ni-doped W (Fig. 1) and explained as segregation-induced GB premelting [13]. It is worth noting that while the importance of GB premelting in unary materials is somewhat controversial, concurrent adsorption in binary or multicomponent systems can in principle stabilize the impurity-based quasi-liquid IGFs over greater undercooling ranges.

A quantitative model has been developed to forecast the thermodynamic stabilization of subsolidus quasi-liquid IGFs in binary alloys [14, 15]. An example computed for Co-doped W is shown in Figure 5. This model calculates the maximum thickness of a stable quasi-liquid IGF without considering interfacial forces, and the computed  $\lambda$  values scale the actual IGF thickness. For ceramic IGFs, additional van der Waals London dispersion forces and electrostatic double-layer interactions can significantly change the film appearance and thickness.

### Interface Transitions and Complexions

Tang, Carter and Cannon demonstrated that GBs in binary alloys can exhibit first-order or continuous transitions that can be interpreted as coupled premelting and prewetting transitions [16].

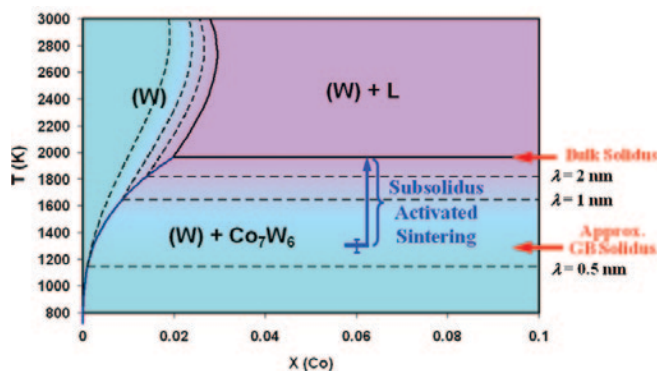


**Figure 5:** A series of dashed lines are drawn in the W-Co binary bulk phase diagram to label the conditions where 0.5-2 nm thick quasi-liquid IGFs can be stable at general GBs in W. Reprinted from Ref. 14 with permission from AIP.

Recently, six distinct GB “complexions” (i.e., interfacial “phases”) with increasing structural disorder were discovered in doped  $\text{Al}_2\text{O}_3$  [17, 18]. As shown in Figure 6, *Complexion I* represents “Langmuir-McLean-like” submonolayer adsorption, *Complexion II* is clean crystalline GBs, *Complexion III* is  $\sim 0.35$  nm thick adsorption double-layers, *Complexion IV* is  $\sim 0.6$  nm IGFs, *Complexion V* is  $\sim 1$ -2 nm thick IGFs, and *Complexion VI* is wetting films. By this scheme, the complexions have been labeled in order of increasing boundary mobility, which varies by 4 orders of magnitude at a particular temperature. Furthermore, the concept of GB complexions and their transitions helps solve an outstanding scientific problem regarding the origin of abnormal grain growth [17, 18].

In a phenomenological thermodynamic model [14, 15], a finite atomic effect can produce a series of discrete GB transitions, leading to the formation of multiple distinct complexions (Figure 7). The concepts of interface transitions and complexions are also applicable to free surfaces, whereas a first-order surface transition from monolayer adsorption to nanoscale SAFs (i.e., a coupled surface premelting and prewetting transition) has indeed been revealed (Figure 2) [7].

### Technological Importance

Nanoscale (equilibrium or meta-stable) SAFs can control the shape, coarsening, and properties of oxide nanoparticles. For example, formation of  $\text{TiO}_2$ -based SAFs can convert polyhedral  $\text{CeO}_2$  into spherical nanoparticles, which is significant for applications as abrasives for chemical-mechanical planarization [19]. In another recent extraordinary example, nanoscale SAFs on  $\text{LiFePO}_4$  nanoparticles are credited as a “fast ion-conducting surface phase,” producing “beltways” for ultrafast charging and discharging of Li ion batteries (in seconds) [20]. Understanding and control of SAFs and their self-selecting thicknesses are also important for tailoring supported oxide catalysts [7] and ultra-thin dielectric films, among many other application areas [1, 5].

In addition to controlling microstructure evolution

(e.g., sintering and grain growth), IGFs and presumably other GB complexions can play critical roles in determining the mechanical properties of  $\text{Si}_3\text{N}_4$ ,  $\text{SiC}$ ,  $\text{Al}_2\text{O}_3$ ,  $\text{ZrO}_2$ , and  $\text{B}_4\text{C}$  based structural ceramics. GB complexions have been exploited to reproducibly grow single crystal sapphire by controlled abnormal grain growth [21]. Furthermore, IGFs control the electronic properties of  $\text{RuO}_2$  based thick-film resistors and ZnO-based varistors, and they affect the thermal conductivity of AlN substrates and the critical current of high  $T_c$  superconductors [1]. Liquid-like GB complexions can also exist in metals (e.g., W-Ni [13] and Cu-Bi [22]) and metal matrix composites (e.g., WC-Co) and critically impact on their embrittlement, sintering, creep, oxidation and corrosion properties. The technological importance of SAFs and IGFs has been reviewed [1].

### Concluding Remarks: A Long-Range Scientific Goal

Nanoscale liquid-like interfacial films can exhibit thermodynamic stability and properties that are strikingly different from their bulk counterparts. Furthermore, interfaces can undergo

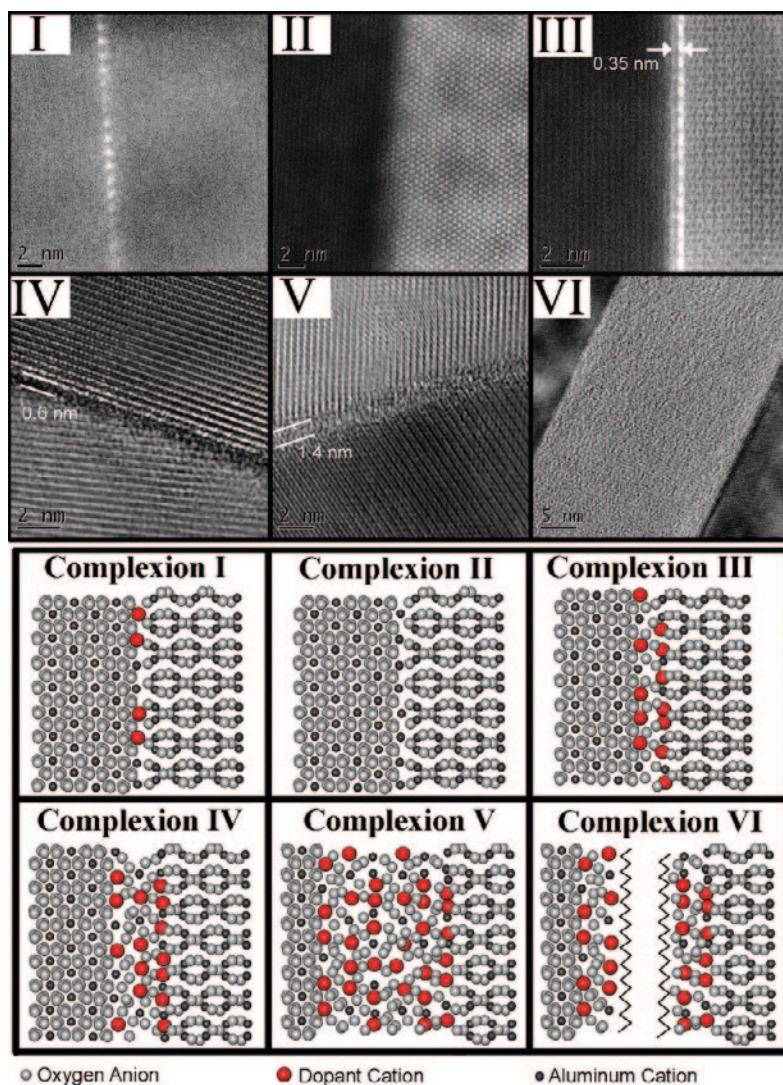


**Figure 6:** HAADF-STEM (I-III) and HRTEM (IV-VI) images of different grain boundary complexions in alumina (top), and representative schematics of each boundary type (bottom). Reprinted from Ref. 17 with permission from Elsevier.

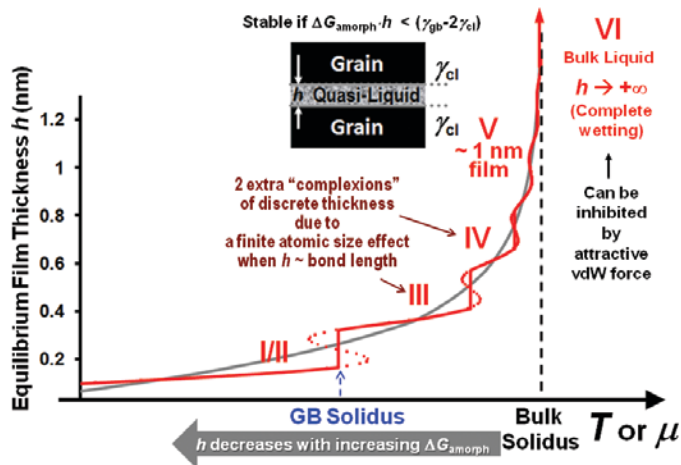


**Figure 7:** A schematic explanation of the physical origins of GB complexions. Stabilization of a subsolidus quasi-liquid intergranular film can be conceived as if the reduced interfacial energy ( $\gamma_{gb} - 2\gamma_{cl}$ ) over compensates the energy penalty to form an undercooled liquid film ( $\Delta G_{ambiphilic} \cdot h$ ), and the film thickness ( $h$ ) decreases with increasing  $\Delta G_{ambiphilic}$ . When the film thickness approaches to the characteristic bond length, a finite atomic size effect can produce a series of GB complexions with discrete thickness. A computed example is represented by the red line, and the corresponding Dillon-Harmer Complexion numbers (I-VI) are labeled. As a reference, the gray line represents the computed film thickness from a continuum model. See Ref. 15 for details.

first-order and continuous transitions. Thus, a long-range scientific goal is to develop quantitative interface complexion (phase) diagrams as a new tool for realizing predictable fabrication of materials by design. For example, the necessity of developing GB diagrams is demonstrated by studies of activated sintering in ceramics [23] and metals [13], showing that short-circuit diffusion in the subsolidus quasi-liquid IGFs leads to accelerated sintering when a bulk liquid phase is not yet stable, with phenomenological similarities to liquid-phase sintering. Thus, bulk phase diagrams are not adequate for designing optimal activated sintering recipes; on the other hand, onset sintering temperatures can indeed be predicted by computed GB diagrams (see, e.g., Figure 5) [14]. The computation shown in Figure 5 represents the first step towards the development of quantitative GB diagrams. Related concepts are elaborated in a recent Current Opinion article [15].

### Acknowledgements

The research on SAFs is supported by an NSF CAREER award (Ceramics Program, Grant No. DMR 0448879), the research on activated sintering in refractory metals and metallic IGFs is supported by an AFOSR Young Investigator award (High Temperature Aerospace Materials Program, Grant No. FA9550-07-1-0125), and the research on the fundamental science of GB complexions and transitions is supported by DOE Basic Energy Science grants (DMSE Electron and Scanning Probe Microscopies Program, Grant No. DE-FG02-08ER46511 for J.L. and Grant No. DE-FG02-08ER46548 for S.J.D. and M.P.H.). **MT**

### References

- [1] J Luo, *Crit. Rev. Solid State Mater Sci* 32 (2007) 67.
- [2] R M Cannon et al., *Z Metallkd* 90 (1999) 1002; *Ceram Trans* 118 (2000) 427.

- [3] J G Dash et al., *Rev Mod Phys* 78 (2006) 695.
- [4] J W Cahn, *J Chem Phys* 66 (1977) 3667.
- [5] J Luo and Y-M Chiang, *Annu Rev Mater Res* 38 (2008) 227.
- [6] R Rosenberg, *Phys Today* 58 (2005) 50.
- [7] H Qian and J Luo, *Acta Mater* 56 (2008) 4702; *Appl Phys Lett* 91 (2007) 061909.
- [8] J Luo and Y-M Chiang, *J European Ceram Soc* 19 (1999) 697.
- [9] J Luo and Y-M Chiang, *Acta Mater* 48 (2000) 4501.
- [10] J Luo et al., *Langmuir* 21 (2005) 7358.
- [11] H J Qian et al., *Acta Mater* 56 (2008).
- [12] D R Clarke, *J Am Ceram Soc* 70 (1987) 15.
- [13] J Luo et al., *Appl Phys Lett* 87 (2005) 231902; V. K. Gupta et al., *Acta Mater* 55 (2007) 3131.
- [14] J Luo and X Shi, *Appl Phys Lett* 92 (2008) 101901.
- [15] J Luo, *Curr Opin Solid State Mater Sci* 12 (2008) 81.
- [16] M Tang et al., *Phys Rev Lett* 97 (2006) 075502.
- [17] S J Dillon et al., *Acta Mater* 55 (2007) 6208.
- [18] S J Dillon and M. P. Harmer, *J European Ceram Soc* 28 (2008) 1485; *J Am Ceram Soc* 91 (2008) 2304; *J Am Ceram Soc* 91 (2008) 2314.
- [19] X Feng et al., *Science* 312 (2004) 1504.
- [20] B Kang and G Ceder, *Nature* (2009) 458.
- [21] S J Dillon and M P Harmer, *J Am Ceram Soc* 90 (2007) 993.
- [22] B B Straumal and B Baretzky, *Interf Sci* 12 (2004) 147.
- [23] J Luo et al., *J Am Ceram Soc* 82 (1999) 916.

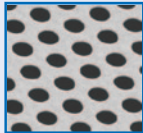
## PELCO®

# Silicon Nitride Membranes


### Next Generation

### Si<sub>3</sub>N<sub>4</sub> TEM Support Films


- Durable and inert planar 50 and 200nm substrates
- 3.0mm circular frame
- EasyGrip™ edges
- Free from debris
- Complimented with Holey Membranes and Silicon Dioxide Substrates



Holey  
Si<sub>3</sub>N<sub>4</sub>  
Membrane



Silicon  
Dioxide  
Membrane



**TED PELLA, INC.**  
Microscopy Products for Science and Industry

sales@tedpella.com 800-237-3526 www.tedpella.com

# So Many Applications, So Many Choices

## Hitachi – the Right Choice

The nano world is more diverse than ever before so why limit your choices. Hitachi offers more choices than any other manufacturer for Ultra High Resolution Field Emission SEM. From the world's highest resolution S-5500 UHR FESEM, guaranteed at 0.4nm resolution to the SU-70 Analytical FESEM capable of producing greater than 200nA beam current, Hitachi's choices are better than ever. Our field proven S-4800 and newly designed SU8000 UHR FESEM with the world's first triple detection system, provide unsurpassed resolution, ease of operation and the most reliable instruments in the industry. Hitachi, the right choice for your application



**S-5500 UHR FESEM**



**SU8000 Triple Detector FESEM**



**S-4800 High Resolution FESEM**



**SU-70 Analytical FESEM**

**HITACHI**  
Inspire the Next